ELSEVIER

Serotype-selective, small-molecule inhibitors of the zinc endopeptidase of botulinum neurotoxin serotype A

Jewn Giew Park,[a] Peter C. Sill,[a] Edward F. Makiyi,[a] Alfonso T. Garcia-Sosa,[a] Charles B. Millard,[b] James J. Schmidt[c],* and Yuan-Ping Pang[a],*

[a]Computer-Aided Molecular Design Laboratory, Mayo Clinic College of Medicine, 200 First Street SW, Rochester, MN 55905, USA
[b]Walter Reed Army Institute of Research, Division of Biochemistry, 503 Robert Grant Avenue, Silver Spring, MD 20910, USA
[c]Department of Cell Biology and Biochemistry, Toxinology and Aerobiology Division, United States Army Medical Research Institute of Infectious Diseases, 1425 Porter Street, Frederick, MD 21702, USA

Abstract—Botulinum neurotoxin serotype A (BoNTA) is one of the most toxic substances known. Currently, there is no antidote to BoNTA. Small molecules identified from high-throughput screening reportedly inhibit the endopeptidase—the zinc-bound, catalytic domain of BoNTA—at a drug concentration of 20 μM. However, optimization of these inhibitors is hampered by challenges including the computational evaluation of the ability of a zinc ligand to compete for coordination with nearby residues in the active site of BoNTA. No improved inhibitor of the endopeptidase has been reported. This article reports the development of a serotype-selective, small-molecule inhibitor of BoNTA with a K_i of 12 μM. This inhibitor was designed to coordinate the zinc ion embedded in the active site of the enzyme for affinity and to interact with a species-specific residue in the active site for selectivity. It is the most potent small-molecule inhibitor of BoNTA reported to date. The results suggest that multiple molecular dynamics simulations using the cationic dummy atom approach are useful to structure-based design of zinc protease inhibitors.
© 2005 Elsevier Ltd. All rights reserved.

1. Introduction

Botulinum neurotoxin serotype A (BoNTA) is a highly toxic by-product of a naturally occurring, spore-forming anaerobic bacterium, *Clostridium botulinum*. BoNTA inhibits the release of acetylcholine from presynaptic nerve terminals at neuromuscular junctions thus causing flaccid paralysis and leading to death by respiratory arrest.[1] BoNTA appears to be effective in treating muscle dysfunctions[2] and has been widely used as a cosmetic known as Botox to temporarily diminish facial lines.[3] However, BoNTA is fatal when misused.[4] Currently, there is no chemical antidote to BoNTA. Small-molecule inhibitors of BoNTA as chemical antidotes are highly desirable.

Development of such antidotes has long been challenging because BoNTA is not a 'drug-friendly' protein.[5] The crystal structure of the holo BoNTA comprises two chains that are linked by a disulfide bond.[6] The light chain (50 kDa) is a zinc endopeptidase (hereafter the endopeptidase) that specifically cleaves neuronal proteins responsible for acetylcholine release.[7] The heavy chain (100 kDa) mediates selective binding to neuronal cells via specific gangliosides and translocates the light chain into the cytosol after receptor-mediated endocytosis of the entire molecule.[8] Although both chains can be used as targets for developing small-molecule antidotes to BoNTA,[9–11] it is technically less challenging to use the light chain as a target for four reasons.

First, a theoretical 3D model of the endopeptidase complexed with a P4–P3′ substrate fragment has been developed and made available at the Protein Data Bank (PDB code: 1UEE, manuscript submitted). This model offers insights into how the substrate interacts with the active-site residues of the endopeptidase and which region of the active site is worth targeting to improve affinity and selectivity of a small-molecule inhibitor of the

endopeptidase. The model suggests that the deep active site of the endopeptidase is filled with a rod-shaped heptapeptide. This structural feature requires that a molecule be at least 10 carbons long to be an effective inhibitor of the endopeptidase. This is consistent with the fact that small-molecule inhibitors reported to date are more than 10 carbons long.[11] The model also suggests that the interaction of Phe193 of the endopeptidase with a substrate or an inhibitor partly establishes specificity of a substrate or selectivity of inhibitors.

Second, there are examples[12,13] to support the notion that the affinities of the small molecules binding at the active site of the endopeptidase could be greatly improved by these molecules' coordination to the zinc ion at the active site. The presence of a zinc ion in the active site of the endopeptidase permits the design of small molecules with affinities that are high enough for these molecules to compete with protein substrates for binding to the endopeptidase. The affinities of the small molecules binding at the heavy-chain domain are, however, difficult to improve to the extent that these molecules can compete with neuronal cells for binding to the heavy-chain domain. This is because the heavy-chain domain lacks a deep pocket at the interface of its complex.[5,9]

Third, the four-ligand coordination of the zinc ion embedded in the active site of the endopeptidase can be computationally simulated with the cationic dummy atom (CaDA) approach[14–18] without resorting to the use of a covalent bond between zinc and its coordinate[19–21] or to semiempirical calculations.[22] This approach uses four identical dummy atoms tetrahedrically attached to the zinc ion and transfers all the atomic charge of the zinc divalent cation evenly to the four dummy atoms. The four peripheral atoms are 'dummy' in that they interact with other atoms electrostatically but not sterically, thus mimicking zinc's $4s4p^3$ vacant orbitals that accommodate the lone-pair electrons of zinc coordinates.[14–18,23] The CaDA approach enables (i) refinement of the endopeptidase, (ii) identification of small molecules that are able to coordinate the zinc ion upon binding to the active site of the endopeptidase via docking and molecular dynamics simulations, and (iii) optimization of the zinc-coordinating molecules via free energy perturbation study.[24]

Fourth, the X-ray structure of an inactive variant of the endopeptidase in complex with a substrate has been reported.[25] In addition to the use of the active site of the endopeptidase as a target described above, the X-ray structure suggests that one can develop selective inhibitors targeting the substrate-interacting surface regions remote to the active site.[25]

Indeed, small peptides and their analogs are able to inhibit the endopeptidase of BoNTA and a closely related zinc endopeptidase of botulinum neurotoxin serotype B (BoNTB) at nanomolar concentrations.[26–30] Recently, a high-throughput screen targeting the endopeptidase of BoNTA has identified small molecules that inhibit the endopeptidase at a drug concentration of 20 μM.[11] However, optimization of such small molecules is hampered by some challenges including the computational evaluation of the ability of a zinc coordinate to compete for zinc coordination with other zinc coordinates in the active site of the endopeptidase. To date, no improved small-molecule inhibitor for BoNTA has been reported.

This article reports the design, synthesis, and testing of serotype-specific small-molecule inhibitors of the endopeptidase of BoNTA. The results provides insights for the development of better antidotes to BoNTA and to the development of other metalloenzyme inhibitors.

2. Results

2.1. Design

A computational screen of a chemical database was first carried out to identify molecules capable of coordination with the zinc ion in the active site of the endopeptidase. This screen was performed using an in-house database of 2.5 million chemical structures and the crystal structure of the zinc-bound endopeptidase[6] according to a published protocol.[31] It had been reported that the interaction energies between zinc and its coordinates were markedly underestimated by molecular mechanics calculations if the zinc ion was modeled traditionally with a one-atom-zinc representation.[32] To minimize the underestimation that would hamper the search of zinc coordinates, the CaDA approach[14–18] was used in the screen to estimate the zinc affinities of potential endopeptidase inhibitors.

The top eight compounds identified in the screen were purchased or synthesized and tested as potential inhibitors of the endopeptidase. Of the eight compounds, compound **1** (Fig. 1) showed 15% inhibition of the endopeptidase at a drug concentration of 100 μM and the rest showed 5–12% inhibition. The reason why only weak inhibitors were identified was in part due to the competition for zinc coordination by a water molecule or neighboring Glu223 in the active site of the endopeptidase, which was supported by subsequent multiple molecular dynamics simulations (MMDSs) described below. The docking-based screen predicts whether or not a functional group such as a carboxylate can coordinate zinc. It does not predict whether the functional group can compete for zinc coordination with a water molecule or Glu223. Therefore, an inhibitor identified from the screen would fail to inhibit the endopeptidase via zinc coordination if its affinity for zinc were lower than that of water or Glu223.

To address this issue 20 different molecular dynamics simulations were carried out for each of the eight computer-identified compounds in complex with the endopeptidase. Each of these simulations was carried out for 2.0 ns with a 1.0-fs time step and different initial velocities using the CaDA approach according to a published protocol.[18,33] Interestingly, only **1** was able to coordinate zinc throughout all 20 simulations; the others failed to coordinate zinc due to the replacement of the zinc coordinate by either a water molecule or the
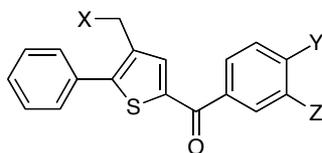
1. X = CO₂H, Y = Cl, Z = H, 15±0(1)% inhibition
2. X = CONHOH, Y = Cl, Z = H, 30±1(2)% inhibition
3. X = CONHOH, Y = Br, Z = H, 11±2(2)% inhibition
4. X = CONHOH, Y = I, Z = NH₂, 40±3(3)% inhibition
5. X = CONHOH, Y = I, Z = NO₂, 3±1(2)% inhibition
6. X = CONHNH₂, Y = Br, Z = H, 5±1(2)% inhibition
7. X = CONHNH₂, Y = I, Z = NH₂, 4±1(2)% inhibition
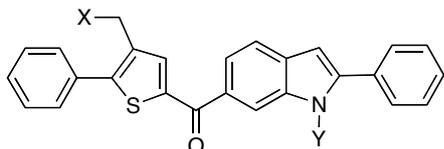
8. X = CO₂H, Y = H, 10±0(2)% inhibition
9. X = CONHOH, Y = H, 4±1(2)% inhibition
10. X = CO₂H, Y = (CH₂)₄NH₂, 30±1(2)% inhibition
11. X = CONHNH₂, Y = (CH₂)₄NH₂, 89±0(2)% inhibition
12. X = CONHOH, Y = (CH₂)₄NH₂, 96±6(2)% inhibition
13. X = CONHOH, Y = (CH₂)₅NH₂, 96±4(2)% inhibition
14. X = CONHOH, Y = (CH₂)₆NH₂, 97±2(2)% inhibition

Figure 1. Chemical structures of inhibitors **1–14** and their inhibition on the zinc endopeptidase of botulinum neurotoxin serotype A at a drug concentration of 100 μM.

carboxylate of Glu223. The correlation between the ability to coordinate zinc in computer simulations and the ability to inhibit the endopeptidase in experiments suggested that MMDSs using the CaDA approach are useful in triaging the docking-identified compounds that have lower affinities for zinc than water and carboxylate.

The MMDSs showed that **1** has a carboxylate coordinating the active-site zinc and a phenyl group interacting with Phe193 of the endopeptidase. This suggested that the affinity of **1** could be improved by strengthening

the zinc coordination using better zinc coordinates such as hydroxamates and its selectivity could be improved by increasing the π–π interaction with Phe193 using additional aromatic rings.

Analog **2** (Fig. 1) with a hydroxamate group as a better zinc ligand[34] was made. A high-pressure-liquid-chromatography-based (HPLC-based) assay showed that **2** is indeed more active in inhibiting the endopeptidase than **1**. Analogs **3–7** (Fig. 1) were made by minor variations of the synthesis of **2**. No MMDS studies were performed on these analogs. In vitro testing revealed that only **4** was more active in inhibiting the endopeptidase than **2**. Without the 3D models of the endopeptidase in complex with **3–7**, respectively, the structure–activity relationship of these analogs offered little guidance in optimization of **2**.

Visual inspection of the MMDS-generated 3D model of the endopeptidase in complex with **1** identified a cavity adjacent to the chlorine-substituted phenyl group of **1**. Given the synthetic feasibility, the chlorine-substituted phenyl ring of **1** was replaced by 2-phenylindole to make a rod-shaped analog **8** (Fig. 1) that satisfies the structural requirement of the endopeptidase inhibitors suggested by the 3D model of a peptide–substrate-bound endopeptidase as described above. MMDSs on the endopeptidase in complex with **8** and its hydroxamic analog **9** (Fig. 1) were performed. The results of these simulations suggested that **8** and **9** were able to fit the active site of the enzyme and coordinate zinc. These compounds were subsequently synthesized and were unexpectedly found to have poor water solubilities. Testing the partially dissolved **8** and **9** showed that both were less potent in inhibiting the endopeptidase than **1** and **2** (Fig. 1).

To increase water solubility and possibly affinity, an aminobutyl group was attached to the indole nitrogen of **9**, which led to the design of **12**. As depicted in Figure 2, MMDSs of **12** showed that: (i) the hydroxamate group was able to coordinate the active-site zinc, (ii)
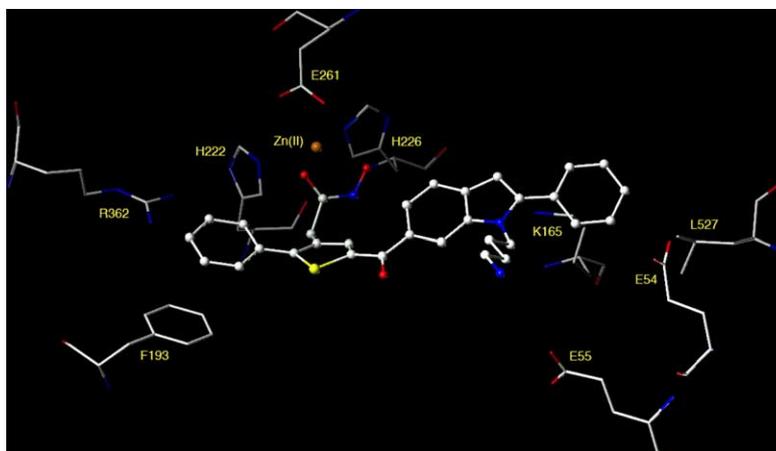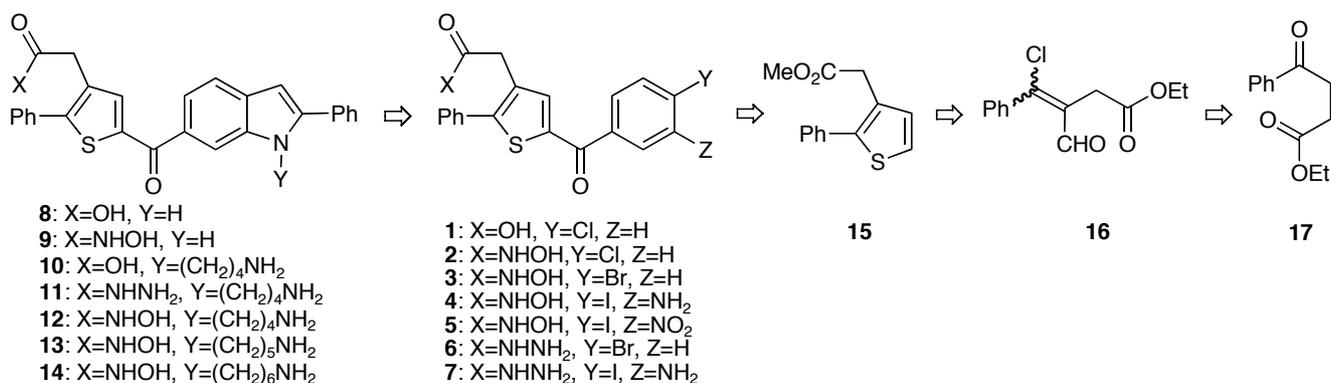

Figure 2. A close-up view of inhibitor **12** (ball-and-stick model) binding at the active site of the endopeptidase of BoNTA (stick model). The 3D structure model was generated by averaging 5000 instantaneous structures obtained at 1.0-ps intervals during the last 500-ps period of 10 molecular dynamics simulations each of which lasted for 2.0 ns with a 1.0-fs time step.

the phenyl group substituted at the thiophene ring had a π–π interaction with Phe193 and a cation–π interaction with Arg362, (iii) the indole ring was engaged in a cation–π interaction with Lys165, (iv) the phenyl group attached to the indole ring has a van der Waals interaction with the side chain of Leu527 and a cation–π interaction with Lys165, and (v) the ammonium group interacted with the carboxylates of Glu54 and Glu55. The energetically favorable 3D model of the **12**-bound endopeptidase prompted for the synthesis and testing of analogs **10–14** (Fig. 1), where **10** is a synthetic precursor of **12**, and **11** is an analog of **12** made by a minor variation of the synthesis of **12** using hydrazine as a known zinc coordinate.[35] Analogs **13** and **14** were also made to probe the amino chain length.
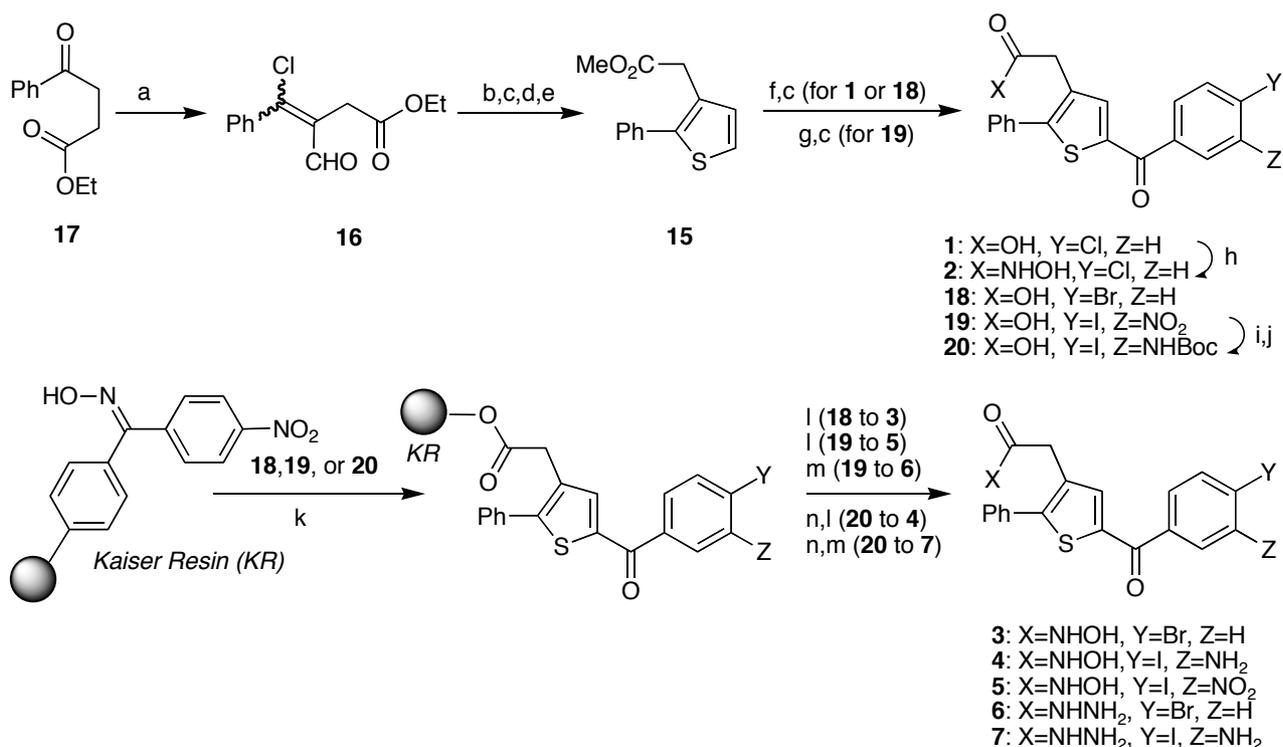
2.2. Synthesis

The retro synthetic analysis for **1–14** is shown in Scheme 1. Compounds **1–7** and compounds **8–14** were prepared in good yields according to Schemes 2 and 3, respectively.

Intermediate **16** was prepared according to a literature procedure.[36–38] To improve the reported yield for **15**,[39] cyclization of **16** to **15** was carried out by the treatment of mercaptoacetic acid and triethylamine in refluxing THF for 4 h followed by removing THF via distillation and heating at 130 °C in DMF for 18 h. The cyclization reaction inevitably produced a UV-inactive, sulfur-containing impurity. This impurity interfered with the

8: X=OH, Y=H
9: X=NHOH, Y=H
10: X=OH, Y=(CH₂)₄NH₂
11: X=NHNH₂, Y=(CH₂)₄NH₂
12: X=NHOH, Y=(CH₂)₄NH₂
13: X=NHOH, Y=(CH₂)₅NH₂
14: X=NHOH, Y=(CH₂)₆NH₂

1: X=OH, Y=Cl, Z=H
2: X=NHOH, Y=Cl, Z=H
3: X=NHOH, Y=Br, Z=H
4: X=NHOH, Y=I, Z=NH₂
5: X=NHOH, Y=I, Z=NO₂
6: X=NHNH₂, Y=Br, Z=H
7: X=NHNH₂, Y=I, Z=NH₂

15 **16** **17**

Scheme 1.

17 **16** **15**

1: X=OH, Y=Cl, Z=H
2: X=NHOH, Y=Cl, Z=H ⎫ h
18: X=OH, Y=Br, Z=H
19: X=OH, Y=I, Z=NO₂
20: X=OH, Y=I, Z=NHBoc ⎫ i,j

3: X=NHOH, Y=Br, Z=H
4: X=NHOH, Y=I, Z=NH₂
5: X=NHOH, Y=I, Z=NO₂
6: X=NHNH₂, Y=Br, Z=H
7: X=NHNH₂, Y=I, Z=NH₂

Scheme 2. Reagents and conditions: (a) DMF/POCl₃; (b) HSCH₂CO₂H/NEt₃/THF and DMF; (c) NaOH/MeOH; (d) purification; (e) HCl/MeOH; (f) 4-Cl/Br-benzoyl chloride/AlCl₃/CH₂Cl₂, rt; (g) 4-iodo-3-nitrobenzoyl chloride/AlCl₃/CH₂Cl₂, rt; (h) NH₂OH·HCl/EDCI/HOBT/NMM/CH₂Cl₂; (i) SnCl₂·2H₂O/EtOAc, reflux; (j) (Boc)₂O/DIEA/DMAP/THF; (k) EDCI/HOBt/NMM/CH₂Cl₂; (l) NH₂OH/CHCl₃; (m) NH₂NH₂/EtOH/THF; (n) TFA/CH₂Cl₂.
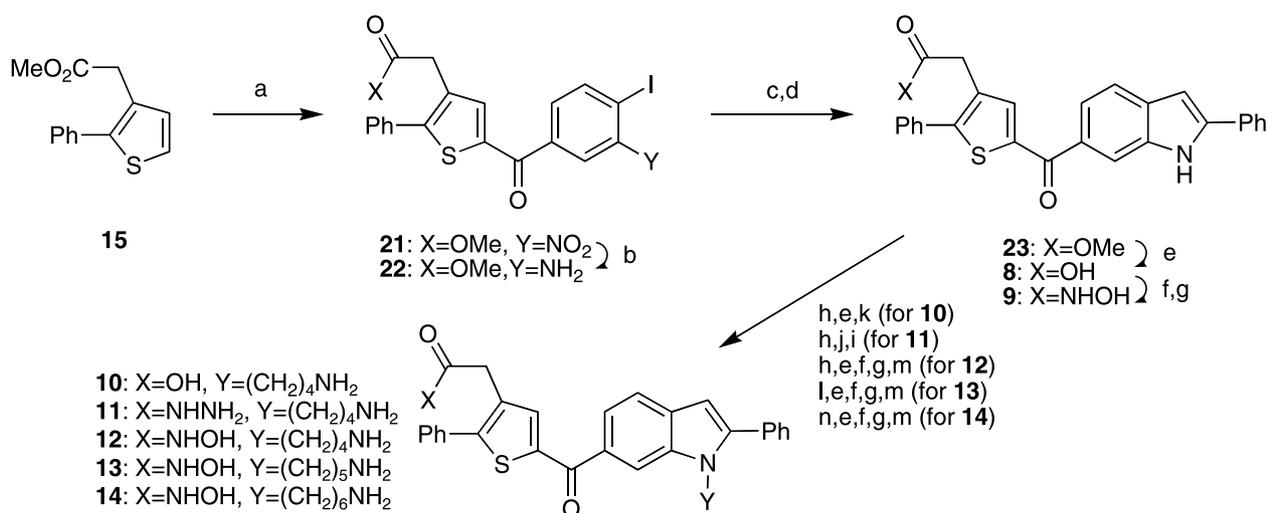
Scheme 3. Reagents and conditions: (a) 4-iodo-3-nitrobenzoyl chloride/AlCl$_3$/CH$_2$Cl$_2$, rt; (b) SnCl$_2$ 2H$_2$O/EtOAc, reflux; (c) PhCCH/Pd(Ph$_3$)$_4$/CuI/ Et$_2$NH; (d) PdCl$_2$(PhCN)$_2$/DMF, 80 °C; (e) NaOH/MeOH; (f) Trt-ONH$_2$/HATU[or HBTU]/HOBt/DIEA/CH$_2$Cl$_2$; (g) AcOH/TFE (1:2); (h) *N*-Boc- 4-bromobutyl-amine/CsF–Celite/CH$_3$CN, reflux; (i) HCl/MeOH; (j) N$_2$H$_4$/EtOH/THF; (k) TMSI/CHCl$_3$; (l) *N*-Boc-5-bromopentyl-amine/CsF– Celite/CH$_3$CN, reflux; (m) concd HCl/EtOAc; (n) *N*-Boc-6-bromohexyl-amine/CsF–Celite/CH$_3$CN, reflux.

subsequent Friedel–Crafts reaction and was inseparable from **15** by common purification procedures such as vacuum distillation or column chromatography. This problem was eventually solved by saponification of the ethyl ester group of **15**. The resulting acid was separated by filtration from the sulfur-containing impurity and then converted to a methyl ester.

Friedel–Crafts acylation of **15**[40,41] yielded **1** and intermediates (**8** and **19**) for making **3–7**. In preparing **19**, the Friedel–Crafts reaction gave two regioisomers of the thiophene ring. The unwanted minor isomer had a 0.01-ppm-downfield shift for the thiophene proton and was readily removed by chromatography. Conversion of **19** to **20** was carried out in 95% yield by reduction with stannous chloride[42] as sulfur was feared to poison the Pd catalyst, followed by protection of the amine function with (Boc)$_2$O.

Reaction of **1** with hydroxylamine hydrochloride readily gave rise to **2**. However, a solid-phase synthesis of hydroxamates using the Kaiser resin[43] turned out to be necessary in converting **18–20** to **3–5**, respectively. The Kaiser resin also was used to convert **19** and **20** to **6** and **7**, respectively.

The indole moiety of **23** was constructed in 61% yield by a two-step literature procedure using (Pd(Ph$_3$)$_4$/CuI/ Et$_2$NH and PdCl$_2$(PhCN)$_2$/DMF).[44] A recently reported one-step procedure[45] had a comparable yield (63%), but its operation was more tedious than that of the two-step synthesis. Precursor **23** was converted to **9** in a high yield by basic hydrolysis followed by coupling with *O*-tritylhydroxylamine. Deprotection of the trityl group was carried out effectively by using a 1:2 mixture of AcOH/ 2,2,2-trifluoroethanol.

Introduction of an aminobutyl group to the indole nitrogen of **23** to make **10–14** was initially problematic, presumably due to the poor nucleophilicity of the indole

nitrogen and the competition for alkylation at the methylene group under basic conditions. Weak bases such as K$_2$CO$_3$/DMF, phase-transfer catalyst (PTC), or K$_2$CO$_3$/ 18-crown-6 failed to yield the desired product. Ultimately, CsF–Celite/CH$_3$CN[46] was found to be effective in *N*- alkylation of **23**. Precursor **10** was lastly converted to **11** and **12** using hydrazine and *O*-tritylhydroxylamine, respectively. Analogs **13** and **14** were then made according to the procedure for **12**.

2.3. Testing

HPLC-based assays[47] were used to measure the inhibition of botulinum neurotoxins (BoNT) by **1–14**. This is because these compounds contain an indole and/or phenyl ring (Fig. 1) that would interfere with fluorescence-based assays of BoNT inhibition.[48]

According to the HPLC-based assays, compounds **1–14** demonstrate inhibition of the endopeptidase of BoNTA at the drug concentration of 100 μM, and hydroxamates are more potent than the corresponding carboxylates or hydrazines (Fig. 1). Furthermore, compounds **2**, **4**, and **12** inhibit the endopeptidase of BoNTA but have no effect on BoNTB (Table 1).

Compounds **12–14** are equally active and they are the most potent of the tested series. Kinetics studies show that the K_i value for the inhibition of the endopeptidase of BoNTA by **12** is 12 ± 2.6 μM (average ± standard

Table 1. Inhibition of the endopeptidase (LC) in botulinum neurotoxin serotypes A and B (BoNTA and BoNTB) by hydroxamate-containing inhibitors

Inhibitor	% Inhibition at 100 μM	
	BoNTA LC	BoNTB LC
2	30 ± 1 (2)	0
4	40 ± 3 (3)	0
12	96 ± 6 (2)	0

deviation). Adding more zinc to the assays, up to 0.1 mM, had no effect on the inhibition by **12** (data not shown), confirming that the inhibition was not due to non-specific metal chelation. This is further supported by the finding that **12** did not inhibit the endopeptidase of BoNTB, even when no additional zinc was present. According to the current literature, **12** has been the most potent and serotype-specific small-molecule inhibitor of the endopeptidase of BoNTA.

3. Discussion

3.1. Toxicity

Hydroxamates are known as promiscuous zinc coordinates[34] as exemplified by matrix metalloprotease inhibitors.[49–52] Therefore, one concern of hydroxamates as inhibitors of the endopeptidase is potential toxicity.

The endopeptidases of BoNTA and BoNTB are closely related.[6,53] Only two residues are different in the active site between the two enzymes: Phe162 and Phe193 in BoNTA correspond to Asn169 and Ser200 in BoNTB. One would expect that the hydroxamate-containing inhibitors of BoNTA would inhibit BoNTB indiscriminately. Interestingly, as a good inhibitor of BoNTA, **12** showed no inhibition on BoNTB (Table 1).

This result confirms that hydroxamates can be selective if they are well crafted according to the active sites of their targets.[54,55] While further experimental studies on the interaction of **12** with other metalloenzymes are necessary, according to Table 1 it is unlikely that **12** interacts with other metalloenzymes. The toxicity concern regarding hydroxamate-containing BoNTA inhibitors is remote, especially when more functional groups are introduced to **12** to further improve its affinity and selectivity.

3.2. New strategy to zinc enzyme inhibitors

Structure-based design of zinc enzyme inhibitors has long been a challenging pursuit for two main reasons. One is that the interaction energies between zinc and its coordinates are markedly underestimated by molecular mechanics calculations using the one-atom-zinc representation.[32] The other is that the four-ligand coordination of zinc identified in X-ray structures of zinc enzymes inevitably changes to a six-ligand coordination during energy minimization or molecular dynamics simulations.[14–17] However, these problems can be solved by using the CaDA approach.[14–18]

The present work demonstrates that the ability of a molecule to coordinate the active-site zinc ion is governed by (i) the fitness of the molecule to the zinc-containing active site, (ii) the intrinsic affinity of the molecule for zinc, and (iii) the competitiveness for zinc coordination relative to nearby zinc ligands available in the active site. The last factor is difficult to address structurally and represents a new challenge of structure-based design of zinc enzyme inhibitors.

The free energy perturbation method[24] is perhaps most effective in assessing the relative free energy of binding to zinc for structure-based design of zinc enzyme inhibitors; however, its application to even a truncated BoNTA endopeptidase that comprises 496 amino acid residues is discouragingly expensive. Alternatively, this work suggests that the competitiveness for zinc coordination can be evaluated by MMDSs using the CaDA approach. It is computationally less expensive than the free energy perturbation method, and yet accounts for the entropy and solvent effects in assessing ligands' ability to compete for zinc coordination. Given the success of **12** as the most serotype-specific and potent small-molecule inhibitor of BoNTA to date, the CaDA-based MMDS strategy appears to be useful to structure-based design of zinc enzyme inhibitors.

4. Conclusions

A novel small-molecule inhibitor of the endopeptidase of BoNTA has been developed according to the zinc-containing active site of the enzyme. This inhibitor selectively inhibits the endopeptidase of BoNTA with a K_i of 12 ± 2.6 uM. It was designed to coordinate the zinc ion embedded in the active site of the enzyme for affinity and to interact with a species-specific residue in the active site for selectivity. It is the most potent and serotype-specific small-molecule inhibitor of BoNTA reported to date. This work suggests that MMDSs using the CaDA approach are useful to structure-based design of zinc protease inhibitors.

5. Methods and materials

Preparation of the zinc- and inhibitor-bound endopeptidase. Limited computing resources required that a truncated endopeptidase (residues 1–429, 453–471, and 497–544) be used in this study. The initial 3D structure of the truncated zinc-containing endopeptidase was taken from an available crystal structure of BoNTA (PDB code: 3BTA)[6] and modified according to a published procedure.[15] The zinc divalent cation in the crystal structure was replaced by the tetrahedron-shaped zinc divalent cation that has four cationic dummy atoms surrounding the central zinc ion.[14] The first-shell zinc coordinates (His222 and His226; and Glu261) were deprotonated as histidinate and glutamate, respectively,[14,15,56–58] Glu260 and Glu350, which form a hydrogen bond with His222 and His226, respectively, were protonated as glutamic acid.[14,15,56–58] All other His residues were protonated as histidinium. Inhibitor **12** was manually docked into the active site according to the **1**-bound endopeptidase complex generated by the EUDOC program.[59] Four sodium ions were added to the surface of the protein to neutralize the protein. The published force field parameters of the tetrahedron-shaped zinc divalent cation[16] were used in energy minimizations and in the following described molecular dynamics simulations, with the exception that the force constants for DZ–DZ and ZN–DZ bonds were changed from 540 to 640 kcal/mol. The RESP charges and force field

parameters of inhibitor **12** were generated by the AN-TECHAMBER module of AMBER 7 program[60] using the structure of **12** optimized at the HF/6-31G* level by the Gaussian 98 Program.[61] A 10,000-step energy minimization was first performed on inhibitor **12** with a positional constraint applied to the rest of the complex. A 50-step energy minimization was then performed on the tetrahedron-shaped zinc divalent cation and **12** with a positional constraint applied to the endopeptidase only. A 100-step energy minimization was lastly performed on the entire complex without any restraint or constraint.

5.1. Virtual screening

Computational screening of an in-house database of 2.5 million chemical structures for inhibitor leads of BoN-TA was carried out according to a published protocol.[31] In this study, the EUDOC program[59] was used on a dedicated terascale computer with 420 Intel Xeon processors (2.2 GHz). A docking box ($3.5 \times 3.5 \times 8.0$ Å^3) was defined in the active site of the zinc-bound endopeptidase that was modified from the crystal structure of BoNTA (PDB code: 3BTA)[6] using the procedure described above. The active-site residues that surrounded the docking box were Ile160, Phe162, Phe193, Thr214, Thr219, His222, Glu223, Arg362, Tyr365, Asp369, and Zn(II). The translational and rotational increments for the screening were set at 1.0 Å and 10° of arc, respectively.

5.2. Multiple molecular dynamics simulations

The multiple molecular dynamics simulations (MMDSs) were performed according to a published protocol[16,33] using the parallel PMEMD module of the AMBER 8 program[60] with the Cornell et al. force field (parm96.-dat)[62] The zinc- and **12**-containing endopeptidase complex was solvated with 14,972 TIP3P water molecules[63] and neutralized with four sodium ions, resulting in a system of 52,993 atoms. The topology and coordinate files of the zinc- and **12**-containing endopeptidase were generated by the LINK, EDIT, and PARM modules of the AMBER5 program.[60] All simulations used (1) a dielectric constant of 1.0, (2) the Berendsen coupling algorithm,[64] (3) a periodic boundary condition at a constant temperature of 300 K and a constant pressure of 1 atm with isotropic molecule-based scaling, (4) the particle mesh Ewald method to calculate long-range electrostatic interactions,[65] (5) iwrap = 1 to generate the trajectories for interaction energy calculations using the EUDOC program,[59] (6) a time step of 1.0 fs, (7) the SHAKE-bond-length constraints applied to all bonds involving the hydrogen atom,[66] and (8) default values of all other inputs of the PMEMD module.

5.3. Synthesis

Melting points are uncorrected. Infrared spectra were record on a Thermo Nicolet Avatar 370 FT-IR. ^{1}H NMR spectra were recorded on Bruker Avance 500 (500 MHz), Bruker Avance 600 (600 MHz), or Varian Mercury 400 (400 MHz), or Varian AM60 (60 MHz)

spectrometers. ^{13}C NMR spectra were recorded on Bruker Avance 500 (125 MHz), Bruker Avance 600 (150 MHz), or Varian Mercury 400 (100 MHz) spectrometers. Chemical shifts are reported in ppm from the solvent resonance as the internal standard. Data are reported as follows: chemical shift, multiplicity (s, single; d, doublet; t, triplet; q, quartet; br, broad; and m, multiplet), coupling constants (Hz), integration, and assignment. Mass spectra were obtained on an HP5973 mass-selective detector with an SIS DIP-MS. Anhydrous THF and CH_2Cl_2 were obtained through activated alumina columns by the Solv-Tech Inc. Anhydrous DMF and CH_3CN were obtained by distillation from CaH_2 under N_2. $POCl_3$ was distilled under N_2 immediately before use. All other commercially obtained reagents were used as received. Flash chromatography was performed on silica gel 60 (EM Science, 230–400 mesh).

5.4. (2-Phenylthiophene-3-yl)acetic acid methyl ester (15)

To a solution of 15.5 mL (3 equiv) of freshly distilled DMF in a flame-dried flask at 5 °C was added 15.5 mL (2.5 equiv) of freshly distilled $POCl_3$ under N_2. The $POCl_3$ mixture was warmed to room temperature followed by adding 13.75 g (66.66 mmol) of ethyl 3-benzoylpropionate (**17**). The resulting mixture was stirred at 80 °C for 16 h, cooled to room temperature, poured onto ice, and basified to pH 6 with solid NaOAc. The organic phase was extracted with EtOAc, washed with a saturated $NaHCO_3$ solution, dried over $MgSO_4$, filtered, and concentrated in vacuo. Kugelrohr distillation (195–200 °C/0.1 mmHg) of the concentrated residue gave 14.84 g (88%) of **16** as a brown oil. The product which consisted of E and Z isomers at a ratio of 2:1 was subjected to next reaction without separation.

To a solution of 50 mL THF was added 5.00 g of **16** (19.79 mmol) followed by adding 2.06 mL (29.68 mmol) of mercaptoacetic acid and 8.27 mL NEt$_3$ (59.36 mmol). The resulting solution was refluxed for 4 h. After the removal of THF by distillation, the residue was dissolved in 50 mL DMF and the resulting solution was heated at 130 °C for 18 h. After DMF was removed in vacuo, the residue was diluted with 50 mL H_2O and extracted with EtOAc. The organic layer was dried over $MgSO_4$, filtered, and concentrated in vacuo. The residue was purified by flash chromatography (EtOAc/Hex 1:4) to give 2.71 g (56%) of (2-phenylthiophene-3-yl)acetic acid ethyl ester as a brown oil: ^{1}H NMR (500 MHz, DCDl$_3$) δ 7.47 (d, J = 7.5 Hz, 2H), 7.42 (d, J = 7.4 Hz, 2H), 7.34 (t, J = 7.4 Hz, 1H), 7.25 (d, J = 5.2 Hz, 1H), 7.08 (d, J = 5.2 Hz, 1H), 4.15 (q, J = 7.1 Hz, 2H), 3.64 (s, 2H), 1.24 (t, J = 7.1 Hz, 3H); ^{13}C NMR (125 MHz, CDCl$_3$) δ 171.2, 140.6, 133.8, 129.7, 129.4, 128.5, 127.7, 124.0, 60.8, 34.5, 14.1.

To a solution of 4.34 g (17.63 mmol) of the above ethyl ester in 50 mL of MeOH was added 1.48 g (26.44 mmol) KOH. The resulting mixture was refluxed for 3 h. Afterward brown precipitates from the mixture were removed by filtration and the filtrate was concentrated in vacuo. The residue was dissolved in 20 mL of H_2O, washed

with 20 mL of EtOAc, and acidified to pH ∼ 2–3 with 1 N HCl. The resulting mixture was extracted with 30 mL EtOAc and the organic phase was dried over $MgSO_4$, filtered, and concentrated in vacuo. The residue was dissolved in 50 mL MeOH followed by adding 1.5 mL of concentrated HCl. The resulting solution was refluxed for 5 h. The solvent was removed in vacuo, and the residue was diluted with 20 mL H_2O, neutralized with a saturated $NaHCO_3$ solution, and extracted with 30 mL CH_2Cl_2. The organic layer was dried over $MgSO_4$, filtered, and concentrated in vacuo. The residue was purified by flash chromatography (EtOAc/Hex 1:4) to give 3.30 g (80%) of **15** as a white solid: mp 29–31 °C; ^{1}H NMR (400 MHz, $CDCl_3$) δ 7.48–7.33 (m, 5H), 7.27 (d, *J* = 5.2 Hz, 1H), 7.07 (d, *J* = 5.2 Hz, 1H), 3.70 (s, 3H), 3.66 (s, 2H); ^{13}C NMR (100 MHz, $CDCl_3$) δ 171.8, 140.7, 133.7, 129.7, 129.4, 129.2, 128.6, 127.8, 124.2, 52.1, 34.2; IR (KBr) cm^{-1} 3113, 2941, 1728.

5.5. [5-(4-Chlorobenzoyl)-2-phenylthiophene-3-yl]acetic acid (1)

To a stirred solution of 0.05 g (0.22 mmol) of **15** and 27 μL (0.22 mmol) of 4-chlorobenzoyl chloride in 5 mL of dry CH_2Cl_2 was added 15 mg (0.11 mmol) of $AlCl_3$ in three portions at room temperature. The resulting mixture was stirred overnight. The reaction mixture was slowly poured onto 5 g of ice and allowed to warm to room temperature. The organic layer was dried over $MgSO_4$, filtered, and concentrated in vacuo. The residue was purified by flash chromatography (EtOAc/Hex 1:9) to give 0.04 g (50%) of [5-(4-chlorobenzoyl)-2-phenylthiophene-3-yl]acetic acid methyl ester as a white solid: ^{1}H NMR (600 MHz, $CDCl_3$) δ 7.84 (d, *J* = 8.2 Hz, 2H), 7.61 (s, 1H), 7.50–7.43 (m, 3H), 3.71 (s, 3H), 3.67 (s, 2H); ^{13}C NMR (150 MHz, $CDCl_3$) δ 186.5, 171.1, 150.1, 140.8, 138.6, 137.3, 136.2, 132.6, 130.5, 129.2, 128.9, 128.8, 128.7, 52.2, 34.1; IR (KBr) cm^{-1} 2949, 1737, 1623; LREIMS $C_{20}H_{15}ClO_3S$ requires 370.04. Found: 370 ([M[+]], 100%), 310 (40%), 139 (59%).

To a stirred solution of 0.15 g (0.40 mmol) of the above ester in a mixture of 2 mL THF and 1 mL H_2O was added 0.60 mL (0.60 mmol) of 1 N NaOH at room temperature. The resulting mixture was refluxed for 3 h. The solvent was evaporated in vacuo. The residue was dissolved in 5 mL H_2O and acidified with 0.11 mL of 1 N HCl to give 0.14 g (100%) of **1** as a pale yellow solid: mp 142–143 °C; ^{1}H NMR (400 MHz, $CDCl_3$) δ 9.75 (br s, 1H), 7.84 (d, *J* = 8.6 Hz, 2H), 7.62 (s, 1H), 7.462 (d, *J* = 8.6 Hz, 2H), 7.46 (m, 5H), 3.71 (s, 2H); ^{13}C NMR (100 MHz, $CDCl_3$) δ 186.6, 176.5, 150.6, 140.9, 138.8, 137.2, 136.1, 132.4, 130.6, 129.7, 129.3, 129.2, 129.1, 128.9, 34.0; IR (KBr) cm^{-1} 3058, 2921, 1715, 1628; LREIMS $C_{19}H_{13}ClO_3S$ requires 356.03. Found: 355 ([M[+]], 100%), 310 (25%), 244 (25%), 139 (42%).

5.6. [5-(4-Bromobenzoyl)-2-phenylthiophene-3-yl]acetic acid (18)

Compound **18** was obtained in 74% yield using 4-bromobenzoyl chloride (from 4-bromobenzoic acid and $SOCl_2$) according to the same procedure as the one used for making **1**. Methyl ester of **19**: ^{1}H NMR (60 MHz, $CDCl_3$) δ 7.71 (m, 4H), 7.61 (s, 1H), 7.47 (m, 5H), 3.71 (s, 3H), 3.67 (s, 2H); LREIMS $C_{20}H_{15}BrO_3S$ requires 413.99. Found: 412 ([M−1[+]], 100%), 413 (80%). **19** as a pale yellow solid: mp 147–150 °C; ^{1}H NMR (400 MHz, $CDCl_3$) δ 7.77 (d, *J* = 8.2 Hz, 2H), 7.66 (d, *J* = 8.2 Hz, 2H), 7.62 (s, 1H), 7.48 (m, 5H), 3.72 (s, 2H); ^{13}C NMR (100 MHz, $CDCl_3$) δ 186.8, 175.5, 150.6, 140.9, 137.3, 136.6, 132.5, 131.8, 130.7, 129.8, 129.3, 129.2, 129.1, 127.4, 33.9; IR (KBr) cm^{-1} 2932, 1714, 1625; LREIMS $C_{19}H_{13}BrO_3S$ requires 399.98. Found: 400 ([M[+]], 100%).

5.7. 2-[5-(4-Chlorobenzoyl)-2-phenylthiophene-3-yl]-*N*-hydroxyacetamide (2)

To a stirred mixture of 30 mg (0.08 mmol) of **1**, 11 mg (0.08 mmol) of *N*-hydroxybenzotriazole (HOBt), 21 mg (0.11 mmol) of 1-ethyl-3-(3′-dimethylaminopropyl)carbodiimide hydrochloride (EDCI·HCl), and 28 mL (0.25 mmol) of 4-methylmorpholine in 5 mL dry CH_2Cl_2 was added 6 mg (0.08 mmol) of $HONH_2 \cdot HCl$ at room temperature. The resulting mixture was stirred overnight and washed with 5 mL of H_2O. The organic layer was dried over $MgSO_4$, filtered, and concentrated in vacuo. The residue was purified by flash chromatography (EtOAc) to give 6 mg (20%) of **2** as a white viscous residue that solidified slowly at room temperature: ^{1}H NMR (400 MHz, DMSO-d_6) δ 10.69 (s, 1H), 8.90 (br s, 1H), 7.86 (d, *J* = 8.6 Hz, 2H), 7.72 (s, 1H), 7.68–7.50 (m, 7H), 3.39 (s, 2H); ^{13}C NMR (100 MHz, DMSO-d_6) δ 185.9, 166.3, 148.8, 139.7, 138.6, 137.4, 136.0, 133.0, 132.3, 130.6, 129.2, 129.2, 129.1, 128.9; IR (KBr) cm^{-1} 3305, 3223, 3060, 2921, 1746, 1631, 1436; LREIMS $C_{19}H_{14}ClNO_3S$ requires 371.04. Found: 371 ([M[+]], 9%), 355 (100%).

5.8. [5-(4-Iodo-3-nitrobenzoyl)-2-phenylthiophene-3-yl]acetic acid (19)

To 3.00 g (10.24 mmol) of 4-iodo-3-nitrobenzoic acid was added 20 mL $SOCl_2$. The resulting solution was refluxed for 2 h. The excess thionyl chloride was removed by distillation. A residual amount of thionyl chloride was removed by N_2 stream and thereafter by high vacuum manifold (0.2 mmHg). The resulting acid chloride was dissolved in 30 mL of dry CH_2Cl_2, followed by adding 2.38 g (10.24 mmol) of **15**. To the resulting mixture was added 5.46 g (40.95 mmol, 4.0 equiv) of $AlCl_3$ in five portions at room temperature. The reaction was monitored by TLC. The completed reaction was quenched by pouring the reaction mixture onto 50 g of ice. The aqueous phase was extracted with 50 mL CH_2Cl_2. The organic layer was dried over $MgSO_4$, filtered, and concentrated in vacuo. The residue was purified by flash chromatography (EtOAc/Hex 1:4) to give 3.86 g (74%) of **21** as a yellow solid: ^{1}H NMR (500 MHz, $CDCl_3$) δ 8.34 (d, *J* = 1.9 Hz, 1H), 8.23 (d, *J* = 8.1 Hz, 1H), 7.76 (dd, *J* = 1.9, 8.1 Hz, 1H), 7.64 (s, 1H), 7.48 (m, 5H), 3.73 (s, 3H), 3.69 (s, 2H); ^{13}C NMR (125 MHz, $CDCl_3$) δ 184.3, 170.9, 152.9, 151.4, 142.5, 139.7, 138.8, 137.8, 132.9, 132.3, 131.0, 129.3, 129.2, 129.0, 125.6, 91.1, 52.3, 34.1.

Saponification of **21** using a stoichiometric amount of 1 N NaOH in a 1:1 mixture of MeOH and THF gave **19** as a yellow solid: mp 100–103 °C; ^{1}H NMR (400 MHz, DMSO-d_6) δ 12.52 (br s, 1H), 7.75 (d, $J = 8.2$ Hz, 1H), 7.72 (s, 1H), 7.52 (m, 5H), 7.21 (d, $J = 1.6$ Hz, 1 H), 6.78 (dd, $J = 1.6$, 8.2 Hz, 1H), 3.66 (s, 2H); ^{13}C NMR (100 MHz, DMSO-d_6) δ 186.7, 171.9, 148.8, 148.4, 139.9, 138.9, 138.6, 138.1, 132.4, 132.3, 129.2, 129.1, 128.7, 117.9, 113.7, 88.5, 34.0; IR (KBr) cm^{-1} 3445, 3357, 2920, 1718, 1694; LREIMS C$_{19}$H$_{12}$INO$_5$S requires 492.95. Found: 492 ([M$^+$], 100%).

5.9. [5-(3-*tert*-Butoxycarbonylamino-4-iodobenzoyl)-2-phenylthiophene-3-yl]acetic acid (20)

To a solution of 5.54 g (10.92 mmol) of **21** in 100 mL EtOAc was added 12.32 g (54.60 mmol, 5.0 equiv) of stannous chloride dihydrate. The resulting mixture was refluxed for 30 min under N$_2$, afterward quenched by pouring onto 100 g of ice, and basified to pH 8 with a saturated NaHCO$_3$ solution. The white milky mixture was filtered through a Celite pad to remove the tin oxides. The organic layer was dried over MgSO$_4$, filtered, and concentrated in vacuo to give 5.02 g (96%) of **22** as a yellow solid: ^{1}H NMR (400 MHz, CDCl$_3$) δ 7.79 (d, $J = 8.2$ Hz, 1H), 7.64 (s, 1H), 7.45 (m, 5H), 7.22 (d, $J = 1.5$ Hz, 1H), 6.97 (dd, $J = 1.5$, 8.2 Hz, 1H), 4.33 (br s, 2H), 3.72 (s, 3H), 3.68 (s, 2H); ^{13}C NMR (100 MHz, CDCl$_3$) δ 187.5, 171.5, 150.3, 147.4, 141.2, 139.3, 137.7, 132.9, 130.7, 129.5, 129.3, 129.2, 120.4, 114.6, 89.2, 52.6, 34.4; IR (KBr) cm^{-1} 3457, 3358, 1734, 1626; LREIMS C$_{20}$H$_{16}$INO$_3$S requires 476.99. Found: 477 ([M$^+$], 100%).

To a solution of 0.25 g (0.53 mmol) of **22** in 5 mL of dry THF were added sequentially 0.07 g (0.05 mmol) DMAP, 0.26 g (1.19 mmol) (Boc)$_2$O, and 0.37 mL (2.21 mmol) DIEA. The resulting solution was stirred at room temperature for 12 h and afterward concentrated in vacuo. The residue was dissolved in a mixture of 2 mL of MeOH and 2 mL THF. To the mixture was added 0.1 mL (1.0 mmol) of 1 N NaOH solution. The resulting solution was stirred at room temperature for 3 h. Afterward the color changed from orange to deep red. After the solvent was removed in vacuo, the residue was dissolved in 10 mL EtOAc and washed with 10 mL of a saturated NH$_4$Cl solution. The organic layer was dried over MgSO$_4$, filtered, and concentrated in vacuo. The residue was purified by flash chromatography (EtOAc/Hex 1:1) to give 0.26 g (86%) of **20**: ^{1}H NMR (400 MHz, CDCl$_3$) δ 8.57 (d, $J = 2.2$ Hz, 1H), 7.90 (d, $J = 8.2$ Hz, 1H), 7.71 (s, 1H), 7.49 (m, 5H), 7.26 (dd, $J = 2.2$, 8.2 Hz, 1H), 6.95 (s, 1H), 3.69 (s, 2H), 1.52 (s, 9H); ^{13}C NMR (100 MHz, CDCl$_3$) δ 186.7, 176.1, 152.4, 150.6, 140.9, 139.1, 139.0, 138.6, 137.8, 132.6, 129.9, 129.2, 129.0, 128.9, 124.6, 120.5, 81.6, 34.4, 28.2; IR (KBr) cm^{-1} 3387, 2978, 1723.

5.10. Solid-phase synthesis of 3–7

Kaiser Oxime PS resin (purchased from Senn Chemicals, Switzerland, 1% DVB, 100–200 mesh, 1.6 mmol/

g) packed in a Macro Kan (from IRORI Inc., San Diego, CA) was loaded with **18–20** according to a literature procedure[43] followed by cleavage with hydroxylamine to make **3**, **4**, and **5** or with hydrazine to make **6** and **7**.

5.11. 2-[5-(4-Bromobenzoyl)-2-phenylthiophene-3-yl]-*N*-hydroxyacetamide (3)

^{1}H NMR (400 MHz, DMSO-d_6) δ 10.68 (s, 1H), 8.89 (s, 1H), 7.81 (d, $J = 8.6$ Hz, 2H), 7.78 (d, $J = 8.6$ Hz, 2H), 7.72 (s, 1H), 7.67 (dd, $J = 1.4$, 8.1 Hz, 2H), 7.54–7.47 (m, 3H), 3.69 (s, 2H); ^{13}C NMR (100 MHz, DMSO-d_6) δ 186.1, 166.3, 148.9, 139.6, 138.6, 136.4, 133.0, 132.3, 131.8, 130.7, 129.21, 129.15, 129.06, 126.4, 32.5; IR (KBr) cm^{-1} 3264, 2914, 1635, 1435; LREIMS C$_{19}$H$_{14}$BrNO$_5$S requires 414.99. Found: 417, 415 ([M$^+$], 5%), 402, 400 ([M–NH$^+$], 100%).

5.12. 2-[5-(3-Amino-4-iodobenzoyl)-2-phenylthiophene-3-yl]-*N*-hydroxyacetamide (4)

Mp >170 °C (decomp); ^{1}H NMR (400 MHz, DMSO-d_6) δ 10.69 (s, 1H), 8.87 (s, 1H), 7.71 (d, $J = 8.2$ Hz, 1H), 7.70 (s, 1H), 7.67 (d, $J = 7.5$ Hz, 2H), 7.51 (m, 3H), 7.17 (d, $J = 2.0$ Hz, 1H), 6.75 (dd, $J = 2.0$, 8.0 Hz, 1H), 3.38 (s, 2H); ^{13}C NMR (100 MHz, DMSO-d_6) δ 186.8, 166.3, 149.0, 148.3, 139.9, 138.8, 138.2, 138.1, 132.8, 132.3, 129.1, 129.0, 117.7, 113.5, 88.2, 32.5; IR (KBr) cm^{-1} 3446, 3358, 3218, 2920, 1654, 1608, 1432.

5.13. 2-[5-(3-Nitro-4-iodobenzoyl)-2-phenylthiophene-3-yl]-*N*-hydroxyacetamide (5)

Mp 147–151 °C; ^{1}H NMR (400 MHz, DMSO-d_6) δ 10.66 (s, 1H), 8.88 (s, 1H), 8.34 (d, $J = 7.8$ Hz, 1H), 8.30 (s, 1H), 7.79 (m, 2H), 7.68–7.50 (m, 5H), 3.39 (s, 2H); ^{13}C NMR (100 MHz, DMSO-d_6) δ 184.4, 166.2, 153.4, 149.7, 141.8, 139.3, 138.9, 138.0, 133.2, 132.9, 132.1, 129.3, 129.2, 129.0, 124.6, 93.4, 32.4; IR (KBr) cm^{-1} 3245, 2922, 1629, 1533, 1433; LREIMS C$_{19}$H$_{13}$I-N$_2$O$_5$S requires 507.96. Found: 508 ([M$^+$], 5%), 493 ([M–NH$^+$], 100%).

5.14. [5-(4-Bromobenzoyl)-2-phenylthiophene-3-yl]acetic acid hydrazide (6)

Mp 157–161 °C; ^{1}H NMR (400 MHz, DMSO-d_6) δ 9.23 (s, 1H), 7.80 (d, $J = 8.4$ Hz, 2H), 7.77 (d, $J = 8.4$ Hz, 2H), 7.72 (s, 1H), 7.67 (d, $J = 7.6$ Hz, 2H), 7.49 (m, 3H), 4.25 (br s, 2H), 3.43 (s, 2H); ^{13}C NMR (100 MHz, CDCl$_3$) δ 186.6, 170.6, 150.3, 140.7, 137.2, 136.3, 132.3, 131.7, 131.6, 130.8, 130.6, 129.1, 129.0, 128.9, 128.8, 127.3, 34.2; IR (KBr) cm^{-1} 3294, 3048, 1635, 1435.

5.15. [5-(3-Amino-4-iodobenzoyl)-2-phenylthiophene-3-yl]acetic acid hydrazide (7)

Mp 159–165 °C; ^{1}H NMR (400 MHz, DMSO-d_6) δ 9.13 (s, 1H), 7.62 (d, $J = 8.0$ Hz, 1H), 7.58 (s, 1H), 7.55 (d, $J = 7.6$ Hz, 2H), 7.37 (m, 3H), 7.05 (s, 1H), 6.62 (d, $J = 7.6$ Hz, 1H), 4.12 (br s, 2H), 3.30 (s, 2H); ^{13}C

NMR (100 MHz, DMSO-d_6) δ 186.9, 168.8, 148.9, 148.3, 139.8, 138.9, 138.2, 133.1, 132.4, 129.1, 128.9, 117.8, 113.5, 88.2, 33.5; IR (KBr) cm^{-1} 3432, 1628, 1431; LREIMS $C_{19}H_{16}IN_3O_2S$ requires 477.00. Found: 477 ([M$^+$], 100%), 446 ([M$-$N$_2$H$_3^+$], 45%), 246 ([C_6H_3(NH$_2$)I$^+$], 100%).

5.16. [2-Phenyl-5-(2-phenyl-1*H*-indole-6-carbonyl)thiophene-3-yl]acetic acid methyl ester (23)

To 0.48 g (1.0 mmol) **22** placed in a flask was added 30 mL Et$_2$NH under stream of N$_2$. The resulting solution was degassed for 20 min with a stream of N$_2$. To this solution was added 164.7 μL (1.5 mmol) of phenyl-acetylene. The resulting solution was then degassed for 5 min followed by adding 20.9 mg (0.11 mmol) of CuI and 0.12 g (0.1 mmol) of Pd(PPh$_3$)$_4$ at room temperature. The resulting mixture was degassed for 10 min and stirred at room temperature for 4 h. The solvent was evaporated in vacuo, and the residue was purified by flash chromatography (EtOAc/Hex 1:4) to give 0.44 g (98%) of [5-(3-amino-4-phenylethynylbenzoyl)-2-phenyl-thiophene-3-yl]-acetic acid methyl ester as a yellow solid: mp 146–148 °C; ^{1}H NMR (400 MHz, CDCl$_3$) δ 7.66 (s, 1H), 7.55 (m, 2H), 7.47 (m, 5H), 7.37 (m, 4H), 7.23 (m, 2H), 4.48 (s, 2H), 3.71 (s, 3H), 3.68 (s, 2H); ^{13}C NMR (100 MHz, CDCl$_3$) δ 187.45, 171.3, 149.9, 147.8, 141.2, 138.7, 137.4, 132.8, 132.1, 131.6, 130.4, 129.3, 128.98, 128.94, 128.7, 128.5, 122.8, 118.8, 114.4, 111.8, 97.2, 85.2, 52.3, 34.2.

A solution of 0.81 g (1.79 mmol) of the above compound in 20 mL of dry DMF was degassed with N$_2$ for 15 min followed by adding 0.14 g (0.36 mmol) of PdCl$_2$(PhCN)$_2$. The resulting mixture was degassed for 10 min, heated at 80 °C for 30 min, cooled to room temperature, diluted with 50 mL of H$_2$O, extracted with 3× 30 mL of EtOAc, and concentrated in vacuo. The residue was purified by flash chromatography (EtOAc/Hex 1:4) to give 0.49 g (61%) of **23** as a bright yellow solid: mp 183–185 °C; ^{1}H NMR (400 MHz, CDCl$_3$) δ 9.50 (s, 1H), 8.19 (s, 1H), 7.79 (d, J = 8.3 Hz, 2H), 7.71 (m, 3H), 7.47 (m, 6H), 7.35 (t, J = 7.1 Hz, 1H), 6.89 (s, 1H), 3.71 (s, 3H), 3.68 (s, 2H); ^{13}C NMR (100 MHz, CDCl$_3$) δ 188.2, 171.5, 149.0, 142.1, 141.9, 137.2, 136.4, 132.95, 132.93, 131.7, 131.5, 130.2, 129.3, 129.1, 128.9, 128.8, 128.4, 125.7, 121.9, 120.0, 113.4, 99.9, 52.3, 34.3; IR (KBr) cm^{-1} 3350, 3054, 2947, 1737, 1596, 1436, 1314; LREIMS $C_{28}H_{21}INO_3S$ requires 451.12. Found: 451 ([M$^+$], 100%).

5.17. [2-Phenyl-5-(2-phenyl-1*H*-indole-6-carbonyl)thiophene-3-yl]acetic acid (8)

To a stirred solution of 0.44 g (0.97 mmol) of **23** in 7 mL MeOH and 7 mL THF was added 1.5 mL (1.5 mmol) of 1 N NaOH solution. The resulting solution was stirred at room temperature for 4 h. The solvent was removed in vacuo, and the residue was diluted with 10 mL H$_2$O, acidified to pH $\sim$ 3 with 1 N HCl, and extracted with 30 mL EtOAc. The organic layer was dried over MgSO$_4$, filtered, and concentrated in vacuo. The residue was purified by flash chromatography (EtOAc/Hex 1:1)

to afford 0.36 g (87%) of **8**: mp 238–240 °C; ^{1}H NMR (400 MHz, DMSO-d_6) δ 12.5 (br s, 1H), 12.04 (s, 1H), 8.00 (s, 1H), 7.93 (d, J = 7.4 Hz, 2H), 7.80 (s, 1H), 7.70 (d, J = 8.2 Hz, 1H), 7.59–7.48 (m, 9H), 7.38 (t, J = 7.1 Hz, 1H), 7.07 (d, J = 1.2 Hz, 1H), 3.69 (s, 2H); ^{13}C NMR (100 MHz, CDCl$_3$) δ 186.6, 172.0, 147.4, 141.6, 141.0, 136.3, 132.6, 132.2, 131.9, 131.4, 130.4, 129.2, 129.1, 128.8, 128.3, 125.6, 125.4, 120.5, 99.3, 34.1; IR (KBr) cm^{-1} 3417, 3054, 1713, 1596.

5.18. *N*-Hydroxy-2-[2-phenyl-5-(2-phenyl-1*H*-indole-6-carbonyl)thiophene-3-yl]acetamide (9)

To a stirred solution of 40.1 mg (0.09 mmol) of **8** in 5 mL of dry CH$_2$Cl$_2$ was added sequentially 140 mg (0.37 mmol) of *O*-(7-azabenzotriazole-1-yl)-*N*,*N*,*N′*,*N′*-tetramethyluronium hexafluorophosphate (HATU), 49.5 mg (0.37 mmol) of HOBt, and 91 μL (0.55 mmol) DIEA. The resulting solution was stirred at room temperature for 10 min followed by adding 50.5 mg (0.18 mmol) of *O*-tritylhydroxylamine. After stirring at the same temperature for 30 min, the solvent was removed in vacuo and the residue was purified by flash chromatography (EtOAc/Hex 1:4) to give *O*-trityl hydroxyamic acid of **8** in a quantitative yield. The resulting oily product was treated with 5 mL of 1:2 mixture of AcOH/2,2,2-trifluoroethanol at room temperature for 24 h. After evaporation of the solvent in vacuo, the residue was dissolved in CH$_2$Cl$_2$ and washed with 10 mL of a saturated NaHCO$_3$ solution. The organic layer was dried over MgSO$_4$, filtered, and concentrated in vacuo. The residue was purified by flash chromatography (MeOH/EtOAc 1:9) to give 12.7 mg (54% over two steps) of **9** as a bright yellow powder: mp $\sim$150 °C (decomp); ^{1}H NMR (400 MHz, DMSO-d_6) δ 12.1 (s, 1H), 11.68 (br s, 1H), 8.95 (br s, 1H), 7.99 (s, 1H), 7.93 (d, J = 7.8 Hz, 2H), 7.81 (s, 1H), 7.70 (m, 3H), 7.66–7.48 (m, 6H), 7.38 (t, J = 7.0 Hz, 1H), 7.08 (s, 1H), 3.41 (s, 2H); ^{13}C NMR (100 MHz, CDCl$_3$) δ 187.4, 167.1, 147.9, 142.3, 141.6, 138.1, 136.9, 133.3, 133.2, 132.8, 132.1, 131.4, 131.0, 129.8, 129.7, 129.0, 127.7, 126.2, 121.1, 120.7, 113.9, 99.9, 33.2; IR (KBr) cm^{-1} 3422–3241, 2902, 1596, 1433, 1322.

5.19. {5-[1-(4-Aminobutyl)-2-phenyl-1*H*-indole-6-carbonyl]-2-phenylthiophene-3-yl}acetic acid hydroiodide (10)

To a stirred solution of 0.20 g (0.45 mmol) of **23** in 10 mL of anhydrous CH$_3$CN was added 1.36 g of CsF–Celite under N$_2$ followed by adding 0.11 g (0.45 mmol) of *N*-Boc-1-bromo-4-butylamine. The resulting mixture was refluxed under N$_2$ for 48 h. The solvent was evaporated under reduced pressure, and the residue was purified by flash chromatography (EtOAc/Hex 1:4) to give 0.07 g (33% based on the recovered starting material) of {5-[1-(4-*N*-Boc-aminobutyl)-2-phenyl-1*H*-indole-6-carbonyl]-2-phenylthiophene-3-yl}acetic acid methyl ester as a yellow foam: ^{1}H NMR (400 MHz, CDCl$_3$) δ 8.04 (s, 1H), 7.73 (m, 3H), 7.50 (m, 8H), 6.60 (s, 1H), 4.51 (br s, 1H), 4.28 (t, J = 6.7 Hz, 2H), 3.72 (s, 3H), 3.70 (s, 2H), 2.97 (m, 2H), 1.73 (q, J = 7.5 Hz, 2H), 1.38 (s, 9H), 1.31 (q, J = 6.3 Hz, 2H); ^{13}C NMR (100 MHz, CDCl$_3$) δ 188.1,

171.5, 155.8, 148.8, 144.9, 142.2, 136.9, 136.6, 132.9, 132.4, 131.7, 131.1, 130.1, 129.3, 128.9, 128.8, 128.7, 128.6, 121.4, 120.2, 112.3, 102.7, 79.1, 52.3, 43.7, 39.9, 34.3, 28.3, 27.4, 27.2; IR (KBr) cm^{-1} 3410–3380, 2930, 1738, 1709, 1625, 1600, 1437.

To a stirred solution of 56.9 mg (9.1×10^{-5} mol) of the above ester in 2 mL MeOH was added 91.4 µL of 1 N NaOH. The resulting mixture was refluxed for 2.5 h. The solvent was removed in vacuo. The residue was diluted with 2.5 mL H_2O, neutralized with 91.4 µL of 1 N HCl, and extracted with 20 mL EtOAc. The organic layer was dried over $MgSO_4$, filtered, and concentrated in vacuo to give 41.3 mg (75%) of {5-[1-(4-*tert*-butoxy-carbonylamino-butyl)-2-phenyl-1*H*-indole-6-carbonyl]-2-phenylthiophene-3-yl}acetic acid as a yellow solid: mp 167–169 °C; ^{1}H NMR (400 MHz, CDCl$_3$) δ 8.00 (s, 1H), 7.73 (m, 2H), 7.49 (m, 11H), 6.60 (s, 1H), 4.14 (t, *J* = 7.0 Hz, 2H), 3.68 (s, 2H), 3.14 (m, 2H), 1.96 (m, 2H), 1.45 (s+m, 9+2H); IR (KBr) cm^{-1} 3433, 3303, 2977, 1714, 1601.

To a stirred solution of 30.0 mg of the above acid (4.93×10^{-5} mol) in 1.0 mL CHCl$_3$ was added 14 µL (9.86×10^{-5} mol) TMSI at room temperature. After stirring at room temperature for 6 h, precipitates were collected by filtration, washed with CHCl$_3$, and dried under high vacuum to give 14.9 mg (47%) of **10** in its HI salt form as a brown powder: mp >150 °C (decomp); ^{1}H NMR (400 MHz, DMSO-d_6) δ 12.9 (br s, 1H), 8.12 (s, 1H), 7.81 (s, 1H), 7.75 (d, *J* = 8.2 Hz, 1H), 7.62–7.49 (m, 11H), 6.71 (s, 1H), 4.36 (t, *J* = 7.0 Hz, 2H), 3.70 (s, 2H), 3.44 (br s, 3H), 2.62 (h, *J* = 5.1 Hz, 2H), 1.65 (m, 2H), 1.29 (m, 2H); ^{13}C NMR (100 MHz, DMSO-d_6) δ 186.9, 172.1, 147.5, 144.5, 140.9, 138.5, 136.2, 132.5, 132.1, 131.8, 131.1, 130.5, 129.2, 129.16, 129.06, 128.9, 128.8, 120.6, 120.2, 112.5, 102.6, 43.1, 38.4, 34.1, 26.7, 24.3; IR (KBr) cm^{-1} 3438, 3057, 1718, 1590; LREIMS $C_{31}H_{28}N_2O_3S$ (neutral form) requires 508.18. Found: 490 ([M$^+$−H$_2$O], 60%).

5.20. {5-[1-(4-Aminobutyl)-2-phenyl-1*H*-indole-6-carbonyl]-2-phenylthiophene-3-yl}acetic acid hydrazide hydrochloride (11)

To a stirred solution of 53.2 mg (8.54×10^{-5} mol) of {5-[1-(4-*N*-Boc-aminobutyl)-2-phenyl-1*H*-indole-6-carbonyl]-2-phenylthiophene-3-yl} acetic acid methyl ester in 1.5 mL MeOH and 1.5 mL THF was added 415 µL of hydrazine hydrate at room temperature. After stirring at room temperature for 4.5 h, the solvent was removed in vacuo. The residue was purified by flash chromatography (EtOAc) to afford 49.7 mg (93%) of acid hydrazide as a yellow foam. To a solution of 60.0 mg of the acid hydrazide (9.6×10^{-5} mol) in 1 mL MeOH was added 16 µL (19.3×10^{-5} mol) of 12 N HCl at room temperature. After stirring at room temperature for 17 h, the solvent was removed in vacuo. The deep red residue was dissolved in 10 mL EtOAc followed by extraction with 5 mL H_2O. The aqueous layer was filtered through a Celite pad. The filtrate was freeze-dried to afford 11.5 mg (20%) of **11** as a dark red-brown powder (dihydrochloride): ^{1}H NMR (400 MHz, DMSO-d_6)

δ 11.35 (s, 1H), 10.3 (br s, 3H), 8.13 (s, 1H), 7.89–7.49 (m, 14H), 6.70 (s, 1H), 4.36 (t, *J* = 7.4 Hz, 2H), 3.74 (s, 2H), 2.62 (m, 2H), 1.68 (m, 2H), 1.35 (m, 2H); ^{13}C NMR (100 MHz, DMSO-d_6) δ 186.9, 168.9, 147.9, 144.6, 141.1, 137.9, 136.2, 132.3, 131.8, 131.3, 131.1, 130.4, 129.2, 129.18, 129.0, 128.9, 128.8, 120.6, 120.3, 112.6, 102.5, 43.2, 38.3, 32.9, 26.8, 24.3; IR (KBr) cm^{-1} 3421, 2936, 1700, 1594, 1446.

5.21. 2-{5-[1-(4-Aminobutyl)-2-phenyl-1*H*-indole-6-carbonyl]-2-phenylthiophene-3-yl}-*N*-hydroxyacetamide hydrochloride (12)

To a stirred solution of 43.0 mg (7.1×10^{-5} mol) of {5-[1-(4-*tert*-butoxycarbonylamino-butyl)-2-phenyl-1*H*-in-dole-6-carbonyl]-2-phenylthiophene-3-yl}acetic acid (*N*-Boc-protected **10**) in 5 mL of dry CH$_2$Cl$_2$ was added sequentially 107.4 mg (2.83×10^{-4} mol) HATU, 38.2 mg (2.83×10^{-4} mol) HOBt, and 70 µL (4.24×10^{-4} mol) DIEA at room temperature. The resulting mixture was stirred at room temperature for 10 min followed by adding 38.9 mg (1.41×10^{-4} mol) of *O*-tritylhydoxylamine. After stirring at room temperature for 30 min, the solvent was removed in vacuo, and the residue was purified by flash chromatography (EtOAc/Hex 1:4) to give 32.0 mg (57%) of *O*-tritylhydroxamate as a yellow foam. The resulting material was treated with 1.5 mL of a mixture of AcOH/TFE (1:2) at room temperature for 48 h. The resulting mixture was concentrated under reduced pressure, and the residue was purified by flash chromatography (MeOH/AcOEt 1:9) to afford 23.2 mg (92%) of the hydroxamate: mp ~95 °C (decomp); ^{1}H NMR (400 MHz, DMSO-d_6) δ 10.72 (s, 3H), 8.90 (s, 1H), 8.11 (s, 1H), 7.82 (s, 1H), 7.45–7.48 (m, 12H), 6.68 (s, 1H), 1.67 (s, 1H), 4.31 (t, *J* = 7.0 Hz, 2H), 3.42 (s, 2H), 2.74 (q, *J* = 6.2 Hz, 2H), 1.58 (p, *J* = 7.4 Hz, 2H), 1.29 (s, 9H), 1.16 (m, 2H); ^{13}C NMR (100 MHz, DMSO-d_6) δ 186.9, 166.4, 155.5, 147.4, 144.6, 140.9, 137.9, 136.2, 132.6, 132.5, 131.9, 130.9, 130.5, 129.1, 129.06, 128.9, 128.8, 128.6, 120.5, 120.2, 112.5, 102.4, 77.4, 43.3, 32.6, 28.2, 27.1, 26.7; IR (KBr) cm^{-1} 3370–3260, 2929, 1677, 1448.

To a stirred solution of 75 mg (0.12 mmol) of 2-{5-[1-(4-*N*-Boc-aminobutyl)-2-phenyl-1*H*-indole-6-carbonyl]-2-phenylthiophene-3-yl}-*N*-hydroxyacetamide in ethyl acetate (3 mL) was added 100 µL (1.2 mmol) of 12 N HCl. The reaction mixture was stirred at room temperature for 30 min. The solvent was removed in vacuo and the residue was then dissolved in water. Some insolubles were observed and were removed by filtration through a pad of Celite. The filtrate was freeze-dried under high vacuum to give 61 mg (91% yield) of the desired product as a fine brown powder; mp >155 °C (decomp); ^{1}H NMR (400 MHz, DMSO-d_6) δ 10.89 (s, 1H), 9.02 (s, 1H), 8.12 (s, 1H), 7.84 (s, 1H), 7.76–7.49 (m, 12H), 6.70 (s, 1H), 4.34 (t, *J* = 6.9 Hz, 2H), 3.45 (s, 2H), 2.64 (h, *J* = 6.4 Hz, 2H), 1.69 (m, 2H), 1.36 (m, 2H); ^{13}C NMR (100 MHz, DMSO-d_6) δ 187.7, 167.4, 148.0, 145.2, 141.8, 138.4, 136.8, 133.3, 133.2, 132.5, 131.7, 131.1, 120.8, 129.7, 129.6, 129.4, 121.2, 121.1, 113.3, 103.3, 43.9, 39.1, 33.2, 27.5, 25.0; IR (KBr) cm^{-1} 3404, 3252, 3053, 2925, 1617, 1586, 1448.

5.22. 2-{5-[1-(5-Aminopentyl)-2-phenyl-1*H*-indole-6-carbon-yl]-2-phenylthiophene-3-yl}-*N*-hydroxy-acetamide hydrochloride (13)

A suspension of 0.37 g (0.81 mmol) of **23**, 0.23 g (0.88 mmol, 1.1 equiv) of *N*-Boc-1-bromo-5-pentyl-amine, and 2.00 g (8.0 mmol, 10 equiv) of CsF–Celite in acetonitrile (15 mL) was refluxed under N_2 for 24 h. The suspension was then allowed to cool to room temperature and filtered through a pad of Cel-ite. The filtrate was concentrated in vacuo and the res-idue was purified by flash chromatography (SiO_2, 4:1 Hex/EtOAc) to give 0.40 g (77% yield) of 2-{5-[1-(5-*N*-Boc-aminopentyl)-2-phenyl-1*H*-indole-6-carbonyl]-2-phenylthiophene-3-yl}acetic acid methyl ester as a yel-low foam. R_f = 0.10 (4:1 Hex/EtOAc); ^{1}H NMR (400 MHz, $CDCl_3$) δ 7.96 (s, 1H), 7.70–7.62 (m, 3H), 7.47–7.34 (m, 10H), 6.52 (s, 1H), 4.37 (br s, 1H), 4.17 (t, *J* = 7.0 Hz, 2H), 3.64 (s, 3H), 3.62 (s, 2H), 2.90 (dt, *J* = 4.7, 5.6, 2H), 1.69–1.62 (m, 2H), 1.34 (s, 9H), 1.28–1.21 (m, 2H), 1.12–1.04 (m, 2H); ^{13}C NMR (100 MHz, $CDCl_3$) δ 188.2, 171.7, 156.2, 149.0, 145.1, 142.2, 137.2, 137.0, 133.2, 133.0, 132.4, 131.9, 131.3, 130.4, 129.6, 129.5, 129.2, 129.1, 129.0, 128.8, 121.7, 120.3, 112.5, 102.8, 52.5, 44.1, 34.5, 30.0, 29.7, 28.6, 24.1; IR (KBr) cm^{-1} 3376, 2929, 2858, 1739, 1708, 1624, 1561, 1513.

To a stirred solution of 0.26 g (0.40 mmol) of the above methyl ester in methanol (20 mL) was added 1.5 mL (1.5 mmol, 3.7 equiv) of 1.0 N NaOH. The resulting solution was stirred under reflux for 4 h and then allowed to cool to room temperature. The solvent was removed in vacuo and the residue was dis-solved in 40 mL EtOAc plus 30 mL water. To this biphasic mixture, 1.5 mL (1.5 mmol) of 1.0 N HCl was added. The phases were separated and the aque-ous phase was washed with 40 mL EtOAc. The organ-ic phases were combined and concentrated in vacuo. The residue was purified by flash chromatography (SiO_2, 1:1 Hex/EtOAc) to give 0.25 g (quantitative yield) of 2-{5-[1-(5-*N*-Boc-aminopentyl)-2-phenyl-1*H*-indole-6-carbonyl]-2-phenylthiophene-3-yl}acetic acid as a yellow foam. R_f = 0.29 (1:1 Hex/EtOAc); ^{1}H NMR (400 MHz, $CDCl_3$) δ 12.58 (br s, 1H) 8.03 (s, 1H), 7.78–7.31 (m, 13H), 6.53 (s, 1H), 4.78 (br s, 1H), 4.11 (t, *J* = 8.0 Hz, 2H), 3.58 (s, 2H), 3.02 (m, 2H), 1.81–1.71 (m, 2H), 1.42 (s, 9H), 1.40–1.34 (m, 2H), 1.18–1.09 (m, 2H); ^{13}C NMR (100 MHz, $CDCl_3$) δ 188.2, 175.5, 159.2, 148.8, 144.8, 143.1, 136.8, 136.4, 133.3, 132.8, 131.8, 130.9, 130.7, 129.7, 129.4, 129.2, 129.0, 128.9, 121.3, 120.3, 113.4, 103.0, 81.4, 64.6, 45.1, 41.3, 34.5, 30.5, 29.9, 28.6, 24.5; IR (KBr) cm^{-1} 3371, 2928, 2856, 1711, 1624, 1533, 1479.

To a stirred solution of 0.22 g (0.35 mmol) of the above acid in DCM (20 mL) were added sequentially 0.15 g (0.39 mmol, 1.1 equiv) of HBTU, 0.11 g (0.39 mmol, 1.1 equiv) of *O*-tritylhydroxylamine, and 0.12 mL (0.68 mmol, 1.9 equiv) of diisopropylethylamine (DIEA). The reaction mixture was stirred at room tem-perature for 1.5 h, and then water (15 mL) and brine (5 mL) were added. The phases were separated and the

aqueous phase was washed with DCM (20 mL). The organic phases were combined and concentrated in vac-uo. The residue was purified by flash chromatography (SiO_2, 2:1 Hex/EtOAc) to give 0.21 g (69% yield) of 2-{5-[1-(5-*N*-Boc-aminopentyl)-2-phenyl-1*H*-indole-6-car-bonyl]-2-phenylthiophene-3-yl}-*O*-tritylhydroxy-acetam-ide as a yellow solid. R_f = 0.39 (2:1 Hex/EtOAc); mp ~110 °C; ^{1}H NMR (400 MHz, $CDCl_3$) δ 7.97 (s, 1H), 7.68–7.18 (m, 23H), 6.56 (s, 1H), 4.37 (br s, 1H), 4.16 (t, *J* = 7.0 Hz, 2H), 3.60 (s, 2H), 2.90 (dt, *J* = 4.7, 5.6, 2H), 1.68–1.59 (m, 2H), 1.33 (s, 9H), 1.29–1.19 (m, 2H), 1.12–1.02 (m, 2H); ^{13}C NMR (100 MHz, $CDCl_3$) δ 188.4, 169.7, 156.2, 147.1, 145.1, 142.2, 137.1, 136.9, 136.8, 136.5, 133.5, 133.2, 132.7, 131.9, 131.3, 130.4, 129.6, 129.4, 129.2, 129.1, 129.0, 128.9, 128.7, 128.4, 128.3, 128.2, 128.1, 127.8, 127.7, 127.4, 121.7, 120.3, 112.6, 103.0, 102.9, 64.2, 49.1, 48.9, 46.1, 44.1, 40.5, 36.5; IR (KBr) cm^{-1} 3349, 2972, 2931, 2863, 1708, 1624, 1479, 1390.

A solution of 0.20 g (0.22 mmol) of the above product in 2:1 mixture of 2,2,2-triflouroethanol/acetic acetic (40 mL) was stirred at room temperature overnight. Then the solvent was removed in vacuo and the resi-due was dried under high vacuum for 1.5 h to get rid of most of the acetic acid. The crude dry residue was then purified by flash chromatography (SiO_2, 1:1 Hex/EtOAc) to give 87 mg (61% yield) of 2-{5-[1-(5-*N*-Boc-aminopentyl)-2-phenyl-1*H*-indole-6-carbonyl]-2-phenyl-thiophene-3-yl}-*N*-hydroxy-acetamide as a yellow sol-id. R_f = 0.15 (1:1 Hex/EtOAc); mp ~223 °C; ^{1}H NMR (400 MHz, $CDCl_3$) δ 9.62 (br s, 1H), 8.51 (br s, 1H), 7.99 (s, 1H), 7.78–7.36 (m, 13H), 6.57 (s, 1H), 4.58 (br s, 1H), 4.21 (t, *J* = 7.0 Hz, 2H), 3.52 (s, 2H), 2.96 (t, *J* = 5.7, 2H), 1.79–1.64 (m, 2H), 1.36 (s, 9H), 1.31–1.23 (m, 2H), 1.14–1.08 (m, 2H); ^{13}C NMR (100 MHz, $CDCl_3$) δ 188.0, 168.2, 156.4, 149.1, 145.0, 143.1, 136.5, 133.0, 132.7, 132.0, 131.1, 130.2, 129.6, 129.2, 129.0, 128.7, 121.4, 120.3, 113.1, 103.0, 79.6, 64.2, 60.8, 44.2, 40.5, 29.9, 28.6, 24.0; IR (KBr) cm^{-1} 3245, 2927, 2856, 1674, 1623, 1533, 1478, 1390.

To a stirred solution of 69 mg (0.11 mmol) of the above product in EtOAc (3 mL) was added 90 μL (1.1 mmol, 10 equiv) of 12 N HCl. The reaction mix-ture was stirred at room temperature for 30 min. The solvent was removed in vacuo and the residue was then dissolved in water. Some insolubles were observed and were removed by filtration through a pad of Celite. The filtrate was freeze-dried under high vacuum to give 54 mg (87% yield) of the desired final product **13** as a fine brown powder; mp ~139 °C (decomp); ^{1}H NMR (400 MHz, DMSO-d_6) δ 10.87 (s, 1H), 8.97 (br s, 1H), 8.08 (s, 1H), 7.82–7.47 (m, 13H), 6.68 (s, 1H), 4.29 (t, *J* = 7.0 Hz, 2H), 3.44 (s, 2H), 3.35 (s, 2H), 2.62 (h, *J* = 6.0, 2H), 1.64–1.58 (m, 2H), 1.45–1.36 (m, 2H), 1.21–1.09 (m, 2H); ^{13}C NMR (100 MHz, DMSO-d_6) δ 187.6, 167.3, 148.1, 145.2, 141.6, 138.6, 136.8, 133.4, 133.2, 132.6, 131.6, 131.0, 129.8, 129.7, 129.6, 129.5, 129.4, 121.2, 121.0, 113.1, 103.1, 39.6, 39.1, 33.2, 29.8, 27.1, 23.7; IR (KBr) cm^{-1} 3395, 2936, 1662, 1616, 1596, 1477, 1380.

5.23. 2-{5-[1-(6-Aminohexyl)-2-phenyl-1*H*-indole-6-carbonyl]-2-phenylthiophene-3-yl}-*N*-hydroxyacetamide hydrochloride (14)

The title compound obtained as a fine brown powder was synthesized according to the procedure for **13** in 78% yield from the Boc-protected precursor; mp >137 °C (decomp); ^{1}H NMR (400 MHz, DMSO-d_6) δ 10.79 (s, 1H), 8.92 (br s, 1H), 8.09 (s, 1H), 7.81–7.48 (m, 13H), 6.68 (s, 1H), 4.32 (t, $J = 7.0$ Hz, 2H), 3.42 (s, 2H), 3.34 (s, 2H), 2.59 (h, $J = 6.0$, 2H), 1.61–1.57 (m, 2H), 1.37–1.31 (m, 2H), 1.11–1.07 (m, 4H); ^{13}C NMR (100 MHz, DMSO-d_6) δ 187.6, 167.2, 148.1, 145.3, 141.5, 138.6, 136.9, 133.4, 133.2, 132.7, 131.7, 131.1, 129.83, 129.79, 129.74, 129.6, 129.4, 121.2, 121.0, 113.1, 103.1, 44.0, 39.2, 33.3, 30.1, 27.4, 26.2, 25.9; IR (KBr) cm^{-1} 3423, 2933, 1655, 1648, 1597, 1560, 1477.

5.24. Botulinum neurotoxin inhibition assays

Assays of BoNT protease activities were done at 37 °C and contained 0.5 mM substrate, 0.5–1.5 µg/mL recombinant BoNT light chain, 40 mM HEPES, and 0.05% Tween, pH 7.3. BoNTA light chain assays also contained 1 mM dithiothreitol, 25 µM $ZnCl_2$, and 0.5 mg/mLbovine serum albumin, while BoNTB light chain assays were supplemented with 1 mM dithiothreitol only. Substrate for BoNTA was a peptide containing residues 187–203 of SNAP-25,[47] while that for BoNTB was residues 60–94 of VAMP.[67] Inhibitors were dissolved in dimethylsulfoxide at 10 times the final assay concentration, then diluted into the assay mixture containing substrate, followed by addition of light chain (i.e., inhibitor and light chain were not preincubated). Assay times and light chain concentrations were adjusted so that less than 10% of the substrate was hydrolyzed. Assays were stopped by acidification with trifluoroacetic acid and analyzed by reverse-phase HPLC as described.[47]

5.25. Determination of K_i

Inhibition of BoNTA light chain by **12** was determined in three independent experiments using eight concentrations of **12** in each. K_i was calculated from slopes of Dixon plots with the equation $K_i = K_m/[(\text{slope})(V_{max})(S)]$, where (S) was the substrate concentration.[68] Kinetic constants for the substrate were taken from reference.[48]

Acknowledgments

References and notes

1. Shapiro, R. L.; Hatheway, C.; Swerdlow, D. L. *Ann. Intern. Med.* **1998**, *129*, 221.
2. Kessler, K. R.; Benecke, R. *Neurotoxicology* **1997**, *18*, 761.
3. Springen, K.; Raymond, J.; Skipp, C.; Scelfo, J.; Smalley, S. *Newsweek* **2002**, 50.
4. Singh, B. R. *Nat. Struct. Biol.* **2000**, *7*, 617.
5. Arkin, M. R.; Wells, J. A. *Nat. Rev. Drug Dis.* **2004**, *3*, 301.
6. Lacy, D. B.; Tepp, W.; Cohen, A. C.; Dasgupta, B. R.; Stevens, R. C. *Nat. Struct. Biol.* **1998**, *5*, 898.
7. Simpson, L. L. *Pharmacol. Rev.* **1981**, *33*, 155.
8. Montecucco, C.; Papini, E.; Schiavo, G. *FEBS Lett.* **1994**, *346*, 92.
9. Eswaramoorthy, S.; Kumaran, D.; Swaminathan, S. *Acta Crystallogr. Sect. D* **2001**, *57*, 1743.
10. Lightstone, F. C.; Prieto, M. C.; Singh, A. K.; Piqueras, M. C.; Whittal, R. M. *Chem. Res. Toxicol.* **2000**, *13*, 356.
11. Burnett, J. C.; Schmidt, J. J.; Stafford, R. G.; Panchal, R. G.; Nguyen, T. L. *Biochem. Biophys. Res. Commun.* **2003**, *310*, 84.
12. Katz, B. A.; Clark, J. M.; Finermoore, J. S.; Jenkins, T. E.; Johnson, C. R. *Nature* **1998**, *391*, 608.
13. McMillan, K.; Adler, M.; Auld, D. S.; Baldwin, J. J.; Blasko, E. *Proc. Natl. Acad. Sci. U.S.A.* **2000**, *97*, 1506.
14. Pang, Y.-P. *J. Mol. Model.* **1999**, *5*, 196.
15. Pang, Y.-P.; Xu, K.; El Yazal, J.; Prendergast, F. G. *Protein Sci.* **2000**, *9*, 1857.
16. Pang, Y.-P. *Proteins* **2001**, *45*, 183.
17. Oelschlaeger, P.; Schmid, R. D.; Pleiss, J. *Protein Eng.* **2003**, *16*, 341.
18. Oelschlaeger, P.; Schmid, R. D.; Pleiss, J. *Biochemistry* **2003**, *42*, 8945.
19. Hoops, S. C.; Anderson, K. W.; Merz, K. M. J. *J. Am. Chem. Soc.* **1991**, *113*, 8262.
20. Ryde, U. *Proteins* **1995**, *21*, 40.
21. Lu, D. S.; Voth, G. A. *Proteins* **1998**, *33*, 119.
22. Berweger, C. D.; Thiel, W.; van Gunsteren, W. F. *Proteins* **2000**, *41*, 299.
23. Roe, R. R.; Pang, Y.-P. *J. Mol. Model.* **1999**, *5*, 134.
24. Pang, Y.-P.; Miller, J. L.; Kollman, P. A. *J. Am. Chem. Soc.* **1999**, *121*, 1717.
25. Breidenbach, M. A.; Brunger, A. T. *Nature* **2004**, *432*, 925.
26. Schmidt, J. J.; Stafford, R. G. *FEBS Lett.* **2002**, *532*, 423.
27. Anne, C.; Blommaert, A.; Turcaud, S.; Martin, A. S.; Meudal, H. *Bioorg. Med. Chem.* **2003**, *11*, 4655.
28. Anne, C.; Turcaud, S.; Quancard, J.; Teffo, F.; Meudal, H. *J. Med. Chem.* **2003**, *46*, 4648.
29. Blommaert, A.; Turcaud, S.; Anne, C.; Roques, B. P. *Bioorg. Med. Chem.* **2004**, *12*, 3055.
30. Sukonpan, C.; Oost, T.; Goodnough, M.; Tepp, W.; Johnson, E. A. *J. Pept. Res.* **2004**, *63*, 181.
31. Perola, E.; Xu, K.; Kollmeyer, T. M.; Kaufmann, S. H.; Prendergast, F. G.; Pang, Y.-P. *J. Med. Chem.* **2000**, *43*, 401.
32. Aqvist, J.; Warshel, A. *J. Am. Chem. Soc.* **1990**, *112*, 2860.
33. Pang, Y.-P. *Proteins* **2004**, *57*, 747.
34. El Yazal, J.; Pang, Y.-P. *J. Phys. Chem.* **2000**, *104*, 6499.
35. Borras, J.; Cristea, T.; Supuran, C. T. *Main Group Met. Chem.* **1996**, *19*, 339.
36. Shvedov, V. I.; Savitskaya, N. V.; Fedorova, I. N. USSR SU753091 1985.
37. Shvedov, V. I.; Fedorova, I. N.; Savitskaya, N. V.; Shvarts, G. Y.; Syubaev, R. D. USSR SU1031165 1985.
38. Shvedov, V. I.; Fedorova, I. N. *J. Org. Chem. USSR* **1991**, *27*, 210.
39. Fedorova, I. N.; Shvedov, V. I.; Silin, V. A.; Baklanova, O. V.; Filitis, L. N. *Pharm. Chem. J.* **1987**, *21*, 772.

40. Gupta, R. R.; Kumar, M.; Gupta, V. *Heterocyclic Chemistry*; Springer: Berlin, 1999, Vol. II.
41. Joule, J. A.; Mills, K.; Smith, G. F. *Heterocyclic Chemistry*, 3rd ed.; Stanley Thornes: Cheltenham, 1998.
42. Bellamy, F. D.; Ou, K. *Tetrahedron Lett.* **1984**, *25*, 839.
43. Thouin, E.; Lubell, W. D. *Tetrahedron Lett.* **2000**, *41*, 457.
44. Arcadi, A.; Cacchi, S.; Marinelli, F. *Tetrahedron Lett.* **1989**, *30*, 2581.
45. Sakai, N.; Annaka, K.; Konakahada, T. *Org. Lett.* **2004**, *6*, 1527.
46. Hayat, S.; Atta-ur-Rahman; Choudhary, M. I.; Khan, K. M.; Schumann, W. *Tetrahedron* **2001**, *57*, 9951.
47. Schmidt, J. J.; Bostian, K. A. *J. Protein Chem.* **1997**, *16*, 19.
48. Schmidt, J. J.; Stafford, R. G. *Appl. Environ. Microbiol.* **2003**, *69*, 297.
49. Abbenante, G.; Fairlie, D. P. *Med. Chem.* **2005**, *1*, 71.
50. Matter, H.; Schudok, M. *Curr. Opin. Drug Discov. Develop.* **2004**, *7*, 513.
51. Brown, S.; Meroueh, S. O.; Fridman, R.; Mobashery, S. *Curr. Top. Med. Chem.* **2004**, *4*, 1227.
52. Yamamoto, M.; Tsujishita, H.; Hori, N.; Ohishi, Y.; Inoue, S. *J. Med. Chem.* **1998**, *41*, 1209.
53. Hanson, M. A.; Stevens, R. C. *Nat. Struct. Biol.* **2000**, *7*, 687.
54. Rossello, A.; Nuti, E.; Orlandini, E.; Carelli, P.; Rapposelli, S. *Bioorg. Med. Chem.* **2004**, *12*, 2441.
55. Rush, T. S.; Powers, R. *Curr. Top. Med. Chem.* **2004**, *4*, 1311.
56. El Yazal, J.; Pang, Y.-P. *J. Phys. Chem. B* **1999**, *103*, 8773.
57. El Yazal, J.; Roe, R. R.; Pang, Y.-P. *J. Phys. Chem. B* **2000**, *104*, 6662.
58. El Yazal, J.; Pang, Y.-P. *J. Mol. Struct. (THEOCHEM)* **2001**, *545*, 271.
59. Pang, Y.-P.; Perola, E.; Xu, K.; Prendergast, F. G. *J. Comput. Chem.* **2001**, *22*, 1750.
60. Pearlman, D. A.; Case, D. A.; Caldwell, J. W.; Ross, W. S.; Cheatham, T. E. III *Comput. Phys. Commun.* **1995**, *91*, 1.
61. Frisch, M. J.; Trucks, G. W.; Schlegel, H. B.; Scuseria, G. E.; Robb, M. A. Gaussian: Pittsburgh PA, 2003.
62. Cornell, W. D.; Cieplak, P.; Bayly, C. I.; Gould, I. R.; Merz, K. M., jr. *J. Am. Chem. Soc.* **1995**, *117*, 5179.
63. Jorgensen, W. L.; Chandreskhar, J.; Madura, J. D.; Impey, R. W.; Klein, M. L. *J. Chem. Phys.* **1982**, *79*, 926.
64. Berendsen, H. J. C.; Postma, J. P. M.; van Gunsteren, W. F.; Di Nola, A.; Haak, J. R. *J. Chem. Phys.* **1984**, *81*, 3684.
65. Darden, T. A.; York, D. M.; Pedersen, L. G. *J. Chem. Phys.* **1993**, *98*, 10089.
66. Miyamoto, S.; Kollman, P. A. *J. Comput. Chem.* **1992**, *13*, 952.
67. Shone, C. C.; Roberts, A. K. *Eur. J. Biochem.* **1994**, *225*, 263.
68. Segel, I. H. *Enzyme Kinetics: Behavior and Analysis of Rapid Equilibrium and Steady State Enzyme Systems*; Wiley: New York, 1975.